

Journal of Materials Chemistry A

Accepted Manuscript



This is an *Accepted Manuscript*, which has been through the Royal Society of Chemistry peer review process and has been accepted for publication.

Accepted Manuscripts are published online shortly after acceptance, before technical editing, formatting and proof reading. Using this free service, authors can make their results available to the community, in citable form, before we publish the edited article. We will replace this *Accepted Manuscript* with the edited and formatted *Advance Article* as soon as it is available.

You can find more information about *Accepted Manuscripts* in the [Information for Authors](#).

Please note that technical editing may introduce minor changes to the text and/or graphics, which may alter content. The journal's standard [Terms & Conditions](#) and the [Ethical guidelines](#) still apply. In no event shall the Royal Society of Chemistry be held responsible for any errors or omissions in this *Accepted Manuscript* or any consequences arising from the use of any information it contains.

ARTICLE

High surface area DPA-hematite for efficient detoxification of bisphenol A via peroxymonosulfate activation

Cite this: DOI: 10.1039/x0xx00000x

Wen-Da Oh,^{a, b} Shun-Kuang Lua,^{a, c} Zhili Dong^c and Teik-Thye Lim^{a, b,*}Received 00th January 2012,
Accepted 00th January 2012

DOI: 10.1039/x0xx00000x

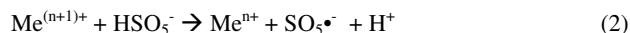
www.rsc.org/

A novel dipicolinic acid-functionalized hematite (DPA-hematite) with high surface area was prepared by co-precipitation of Fe(III)-DPA complex. It was used as a catalyst to activate peroxymonosulfate (PMS) for bisphenol A (BPA) detoxification. The XRD, FESEM, TEM and FTIR characterization indicated that nano-sized DPA-hematite with aggregated quasi nanosphere morphology was obtained with 1:1 ratio of Fe(III) to DPA. Higher catalytic activity of DPA-hematite over other Fe(III)-based catalysts was observed for BPA oxidation in the presence of oxone. The kinetics of BPA removal was investigated using a kinetic model with BPA concentration, initial oxone dosage and surface area of DPA-hematite. For the first time, the acute toxicity of BPA solution over time with elimination of oxone toxicity interference was conducted using *Vibrio fischeri* bacteria and the results indicated that the evolution of acute toxicity was highly dependent on the initial oxone dosage. Under deficit oxone conditions, BPA was completely transformed to by-products along with decreased intrinsic toxicity but ring-opening reactions were barely observed which can be explained based on the dimerization-mineralization degradation pathways. Under excess oxone conditions, the intrinsic toxicity of BPA solution decreased along with ring-opening reactions leading to a greater extent of mineralization. The DPA-hematite can be reused for BPA detoxification for at least three cycles in the presence of 2.0 g L⁻¹ of oxone.

1. Introduction

Bisphenol A (BPA) has been found ubiquitously in treated effluents and natural water systems due to its widespread usage as a monomer in the production of polycarbonate resins and plastics for various applications.^{1,2} BPA is widely known as an anthropogenic endocrine disruptor due to its ability to bind with the estrogen receptor thus inducing feminization in various aquatic organisms.^{3,4} To date, various treatment methods have been proposed to address water contamination due to BPA such as adsorption,⁵ biological treatment,^{6,7} ozonation,⁸ wet air oxidation⁹ and photocatalytic treatment¹⁰. However, these methods suffer from at least one of the disadvantages of high energy requirement, slow process, high cost and generating secondary waste stream.

Recently, sulfate radical based-advanced oxidation processes (S-AOPs) emerged as an environmentally-friendly and potentially-cost effective technology for water pollution abatement. Compare to the hydroxyl radical (OH•, E° = 1.9-2.7 V versus NHE, t_{1/2} = 10⁻³ μs), sulfate radical (SO₄•⁻, E° = 2.5-3.1 V vs NHE, t_{1/2} = 30-40 μs) is longer-lived and more selective in oxidation owing to its preferential oxidation pathway through the electron transfer reaction.^{11,12} In general, SO₄•⁻ can be generated homogeneously or heterogeneously from the activation of peroxymonosulfate (PMS, HSO₅⁻) by transition metals (Me, e.g.: Fe, Cu, Co and Mn) as follows:



To avoid having to recover the catalysts, the heterogeneous system is desirable over the homogeneous system. The discovery of Co(II) as a prominent PMS activator has resulted in tremendous research interests to produce a myriad of efficient Co-based catalysts as PMS activators.¹³⁻¹⁸ However, due to the toxic nature and excessive Co leaching during the catalytic reaction, it is prohibitive to employ Co-based catalyst for water treatment. As alternatives to Co-based catalysts, various environmentally-friendly catalysts with their main framework consisting of the either Fe, Mn or Cu have been developed.¹⁹⁻²² Of all, Fe(III)-based catalysts show promising merits of being eco-friendly, nontoxic and inexpensive materials for catalysis. However, to date, relatively few studies reported on the effective use of Fe(III) catalysts as PMS activators, and they were often considered less effective compared with the Co-based catalysts.²³⁻²⁵ The performance of Fe(III) catalysts can be improved by having higher surface area and introduction of surface functionality.

Herein, a facile co-precipitation synthesis was designed to prepare dipicolinic acid-functionalized hematite (DPA-hematite) with high surface area using Fe-DPA⁺ for BPA (Fig. 1b) detoxification via PMS activation. The synthesis procedure was carried out using gentle heating and environmentally-benign chemicals. DPA or pyridine-2,5-dicarboxylic acid (Fig. 1a) is a nontoxic organic compound and can be found naturally as one of the

main components of the bacterial endospore. It is also amphoteric and consists of functional groups with electron-rich nitrogen and oxygen. Previously, it was reported that DPA is an efficient electron transport mediator that can form complexes with Fe^{3+} to produce effective catalyst for various biomimetic oxidation processes.²⁶⁻²⁹ It is believed that the surface Fe-DPA^+ complex could be established from this synthesis approach and leads to the improved rate of $\text{SO}_4^{\bullet-}$ generation from PMS. For the first time, the acute toxicity of degradation products of BPA at different initial oxone dosages were evaluated in the heterogeneous PMS system which was not due to the intrinsic toxic effect of PMS. The effects of several operational parameters (pH, DPA-hematite loading and oxone dosage) on the performance of the DPA-hematite and its reusability for BPA removal with oxone were also evaluated.

2. Experimental

2.1 Chemicals

All the chemicals used in this study were of analytical grade and were used without further purification. The chemicals were iron(III) chloride (FeCl_3 , Sigma-Aldrich), urea ($\text{CO}(\text{NH}_2)_2$, Hanawa), dipicolinic acid ($\text{C}_7\text{H}_5\text{NO}_4$, Sigma-Aldrich), bisphenol A ($\text{C}_{15}\text{H}_{16}\text{O}_2$, Sigma-Aldrich), cobalt (II,III) oxide (Co_3O_4 , Alfa Aesar), methanol (CH_3OH , Merck), sodium sulfite (Na_2SO_3 , Sigma-Aldrich), acetonitrile ($\text{C}_2\text{H}_3\text{N}$, Merck), potassium iodide (KI, Fisons), potassium peroxymonosulfate in the form of oxone ($2\text{KHSO}_5 \cdot \text{KHSO}_4 \cdot \text{K}_2\text{SO}_4$, Alfa Aesar), commercial goethite (FeOOH , Sigma-Aldrich), commercial hematite (Fe_2O_3 , Alfa Aesar) and sodium hydroxide (NaOH , Alfa Aesar). All the experiments were conducted using the deionized water (18.2 M Ω cm).

2.2 Preparation of DPA-hematite

The DPA-hematite catalyst was prepared by urea assisted co-precipitation of Fe-DPA^+ complex. In a typical experimental procedure, 3 mmol of FeCl_3 and 3 mmol of DPA were dissolved in 80 mL of the deionized water to form a greenish solution consisting of Fe-DPA^+ complex. Then, 30 mmol of urea was added into the above solution and the reaction mixture was gradually heated to 90 °C under vigorous stirring for 24 h. Under this condition, urea decomposed to ammonia and this leads to the precipitation of Fe-DPA^+ complex to form DPA-hematite. The DPA-hematite was separated from the supernatant through centrifugation at 10 000 rpm for 10 min and washed several times with the deionized water. Finally, the DPA-hematite was dried in an oven at 60 °C for 12 h and stored in a desiccator prior to use. The ratios of Fe(III) to DPA were varied at 1:0, 1:1, 1.5:1 and 2:1 during the preparation process.

2.3 Characterization techniques

The X-ray diffraction diffractometer (Bruker D8 Advance XRD) operating on a $\text{Cu-K}\alpha$ X-ray source ($\lambda=1.5418 \text{ \AA}$) at 40 kV and 40 mA was used to characterize the crystal structure of DPA-hematite. The surface morphology and size of DPA-hematite were examined using a field emission scanning electron microscope (FESEM JEOL 7600F) and transmission electron microscope (TEM JEM-2010F). The Brunauer–Emmett–Teller (BET) specific surface areas were determined using the N_2 adsorption-desorption isotherm analysis at 77 K (QuantaChrome Autosorb-1 Analyzer). The fourier transform infrared spectrometer (Perkin Elmer) was used to characterize the surface functional groups of DPA-hematite. The point of zero charge

(pH_{zpc}) of DPA-hematite was determined using a Zetasizer (Malvern).

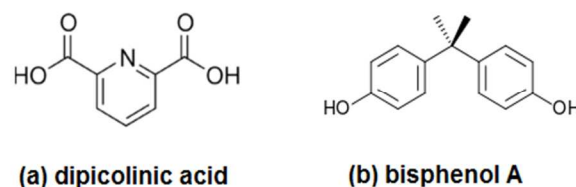


Fig 1. Chemical structure of (a) dipicolinic acid and (b) bisphenol A

2.4 Experimental procedure for BPA degradation and kinetics

The catalytic oxidation of BPA was evaluated at room temperature ($25 \pm 1 \text{ }^\circ\text{C}$) in a 500-mL reaction vessel. In a typical experimental procedure, 200 mL of solution containing 15 mg L^{-1} of BPA was prepared and added into the reaction vessel containing 0.4 g of oxone. Then, the pH of the solution was adjusted to $\text{pH } 7 \pm 0.2$ using 1 M of NaOH and the reaction was immediately commenced under vigorous stirring with the addition of 0.1 g of DPA-hematite into the solution. No adsorption-desorption equilibrium time was allowed as preliminary studies had showed that less than 5% of BPA was removed via adsorption in 24 h. At predetermined time intervals, 1 mL of aliquots from the solution was filtered using a cellulose acetate filter. Then, methanol, which contains α -hydrogen that can react readily with sulfate and hydroxyl radicals, was immediately added into the aliquots to quench the reaction. A control containing only oxone and BPA without catalyst was also carried out. The performance of DPA-hematite was compared with different catalysts, namely the synthesized akaganeite and commercial goethite and hematite. The effects of initial pH (2.5-9.0), DPA-hematite loading (0.25-1.0 g L^{-1}) and initial oxone dosage (0.5-2.0 g L^{-1} corresponding to BPA to oxone molar ratio from 1:12.5 to 1:50) were also investigated. All the degradation experiments were conducted in triplicate. For experiments conducted at various initial oxone dosages and 0.5 g L^{-1} of DPA-hematite, the total organic carbon (TOC), residual PMS concentration and acute toxicity of the treated solution at various reaction times were also determined. Additionally, homogeneous experiments were also carried out following the above-mentioned procedure but using the dissolved Fe-DPA^+ , Fe(III) and DPA at 0.2 mmol L^{-1} as the catalysts.

2.5 Acute toxicity study

The acute toxicity of BPA and its by-products produced during the catalytic reaction was evaluated by measuring the effect of the toxicity of sample towards the bioluminescence of standard *Vibrio fischeri* (NRRL number: B11177) using a Microtox Model 500 Analyzer (Azur Environment, Workingham, England). It is well established that in the presence of toxicity, the rate of respiration and metabolism of *V. fischeri* will be inhibited thus leading to the decrease of its bioluminescence. The *V. fischeri* bacteria was obtained in a freeze-dried form and stored in a freezer at $-20 \text{ }^\circ\text{C}$ prior to use. To reactivate the bacteria for acute toxicity study, reconstitution solution containing sterilized NaCl solution was used. Due to the toxic effect of oxone to the *V. fischeri*, the sample was initially treated with Na_2SO_3 to convert all the HSO_5^- ions to innocuous sulfate ion. Then, the sample pH was adjusted to $\text{pH } 6-7$ using 1 M of NaOH and the osmolality adjusted to 2% using 22% NaCl solution. Measurements of the bioluminescence of *V. fischeri* were carried out at 5, 15 and 30-min of incubation times at 15 °C and

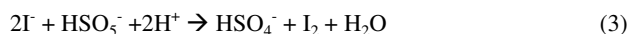
the percentage inhibition (%) was calculated from the MicrotoxOmni software.

2.6 Reusability of DPA-hematite

The reusability of DPA-hematite for BPA detoxification was investigated up to three cycles under the following conditions: 2.0 g L⁻¹ of oxone, 15 mg L⁻¹ of initial BPA concentration, 0.5 g L⁻¹ of DPA-hematite, initial pH of 7 over 240 min run-time. After each cycle, the spent DPA-hematite was recovered through centrifugation at 10 000 rpm for 5 min and dried in an oven at 60 °C for 12 h. Then, the spent catalyst was reused under the same condition as stated above and in each cycle, the BPA concentration, TOC and acute toxicity were determined at t = 240 min. Each of the experiments was conducted in triplicate.

2.7 Analytical methods

The BPA concentration was quantified using a high performance liquid chromatography (Perkin Elmer) with a UV detector at the wavelength of 220 nm. A reversed phased column (Hypersil GOLD) was used with the mobile phase consisting of 60 % acetonitrile to 40 % deionized water at the flow rate of 1 mL min⁻¹. The total organic carbon (TOC) was measured using a TOC analyzer (Shimadzu ASI-V TOC analyzer). For HSO₅⁻ quantification, 5 mL of the sample was initially mixed with 1 g of KI and vigorously shaken for 30 min to allow the oxidation of I⁻ by HSO₅⁻ as follows:



The concentration of I₃⁻, which is directly proportional to PMS, was determined from a calibration curve by using a UV-Vis spectrophotometer at λ_{max} = 352 nm. Several organic acids, namely formic, oxalic and acetic acids were detected using an ion chromatography (Dionex ICS-2100).

3. Results and discussions

3.1 Characterization of DPA-hematite

The schematic illustration of the DPA-hematite synthesis process is presented in Fig. 2. During the synthesis, it was postulated that the Fe-DPA⁺ complex (K_d = 227 M)³⁰ was slowly dissociated to mobile Fe³⁺ ions, which subsequently hydrolysed to goethite and then dehydrated to DPA-hematite under basic condition. From this synthesis approach, DPA functional groups which contain electron-rich nitrogen and oxygen groups can be introduced as the surface-complex on DPA-hematite. Preliminary results showed that DPA can improve the catalytic activity of Fe³⁺ after complexation as observed by the significantly better performance of the homogeneous Fe-DPA⁺/PMS system vis-à-vis the Fe³⁺/PMS system in BPA removal (see Fig. 3). This was because the complexation of DPA to Fe(III) induced chemical shift through (i) the transfer of the unpaired electron spin density from the paramagnetic Fe(III) into ligand orbitals, (ii) the unpaired electron spin polarization, and/or (iii) the dipolar interactions.³¹ The chemical shift is dependent on the type of ligand present and can induce significant changes in the redox potential of Fe(II)/Fe(III) leading to different degrees of promotional effects on the catalysis reaction.^{24, 32}

Figure 4 shows the XRD patterns of the as-prepared Fe nanocatalysts synthesized with and without DPA. The XRD pattern

of the Fe nanocatalyst prepared without DPA (Fe:DPA ratio of 1:0) was indexed to the akaganeite phase (FeOOH/Cl) with no impurity peak. The presence of Cl in the akaganeite was due to the use of FeCl₃ as the precursor during synthesis. However, for samples prepared with Fe(III)-to-DPA ratio of 1.5:1, peaks at 2θ = 24°, 33°, 37°, 41°, 49° and 54° appeared which can be indexed as coming from DPA-hematite. The quantitative Rietveld analysis shows that akaganeite and DPA-hematite phases were coexisted at the percentages of 35 and 65%, respectively. When the Fe(III)-to-DPA ratio was 1:1, the peaks associated with akaganeite disappeared and pure DPA-hematite was obtained.

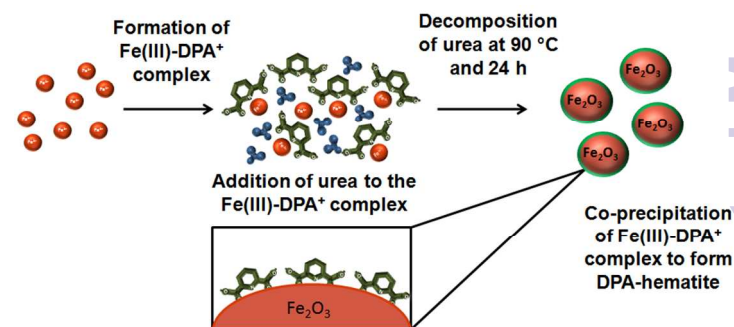


Fig 2. Schematic illustration of the synthesis of DPA-hematite.

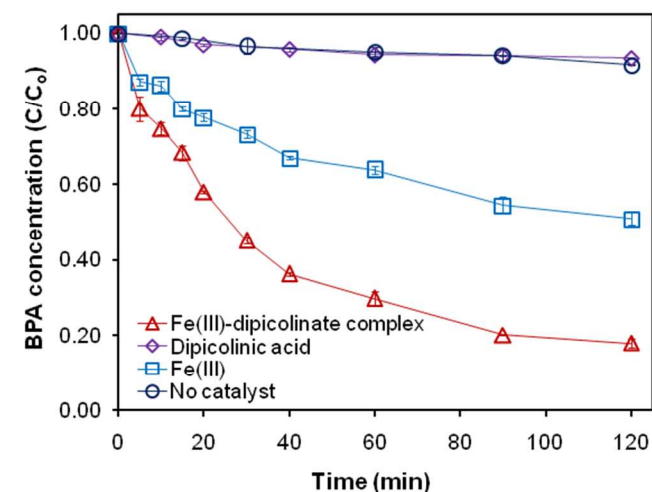


Fig 3. Degradation of BPA by oxone activated by Fe-DPA⁺, Fe(III) and DPA. Conditions: [BPA]₀ = 15 mg L⁻¹, [Oxone]₀ = 2 g L⁻¹, pH₀ = 7 and [catalyst]₀ = 0.2 mmol L⁻¹.

The morphologies of akaganeite and DPA-hematite are as shown in FESEM and TEM images (Fig. 5). The akaganeite formed nanorod-like structure with an average length of 30-60 nm and had a BET specific surface area of 120 m² g⁻¹ while DPA-hematite was consisted of aggregated quasi nanosphere morphology with average diameter between 10-15 nm and the BET specific surface area of 188 m² g⁻¹. The relatively larger specific surface area of DPA-hematite than that of other reported hematite catalyst (34 m² g⁻¹) for PMS activation²³ was favorable for the heterogeneous catalysis.

Figure 6a shows the FTIR spectrum of a typical akaganeite which was synthesized without DPA in which the characteristic absorbance peaks are at about 1500-1700 cm⁻¹ and 600-900 cm⁻¹.³³ For the FTIR spectrum of DPA-hematite (Fig. 6b), the peak at about

1700 cm^{-1} can be ascribed to carboxylic C=O stretching while the peaks at 1300-1500 cm^{-1} could probably be attributed to the asymmetric C=O stretching in COO⁻ group. A broad peak was observed at 600 cm^{-1} which can be indicative of Fe-O bond. These results provide evidence of the presence of DPA functional groups on the surface of DPA-hematite.

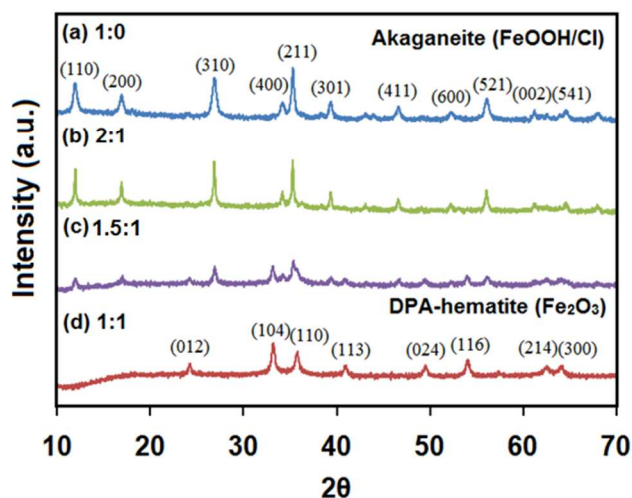


Fig 4. X-ray diffraction patterns of the catalysts synthesized at different ratios of Fe to DPA, indicating that pure DPA-hematite can be prepared using DPA:Fe molar ratio of 1:1.

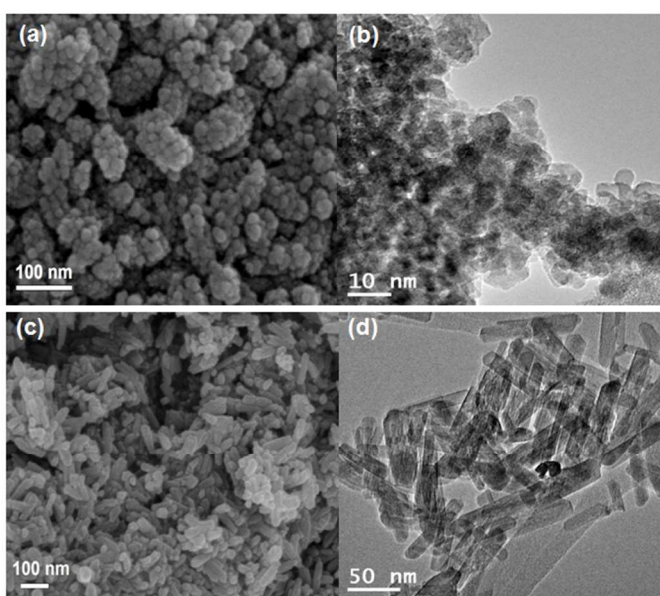


Fig 5. FESEM and TEM images of akaganeite (a and b) and DPA-hematite (c and d).

3.2 Efficiency and kinetics of BPA degradation

3.2.1 Effects of different heterogeneous Fe(III) catalysts and initial pH

Figure 7a shows comparison of the time courses of BPA degradation by different heterogeneous Fe(III) catalysts in the presence of 2.0 g

L^{-1} of oxone. The control experiment containing BPA and oxone without catalyst showed ~8% reduction in BPA concentration over 120 min. This signifies that BPA is difficult to be degraded by PMS

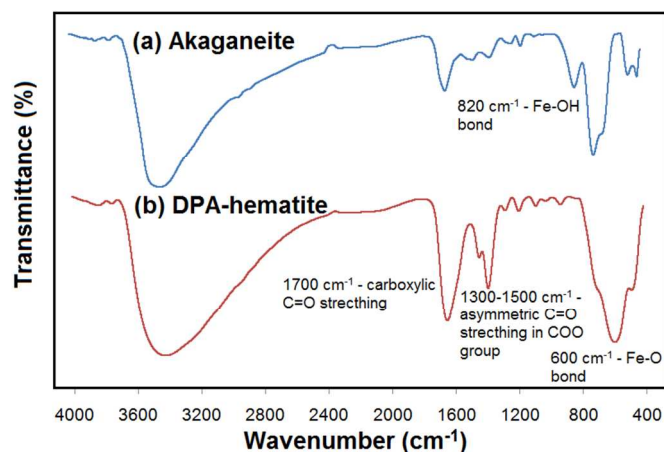


Fig 6. FTIR spectra of (a) akaganeite and (b) DPA-hematite.

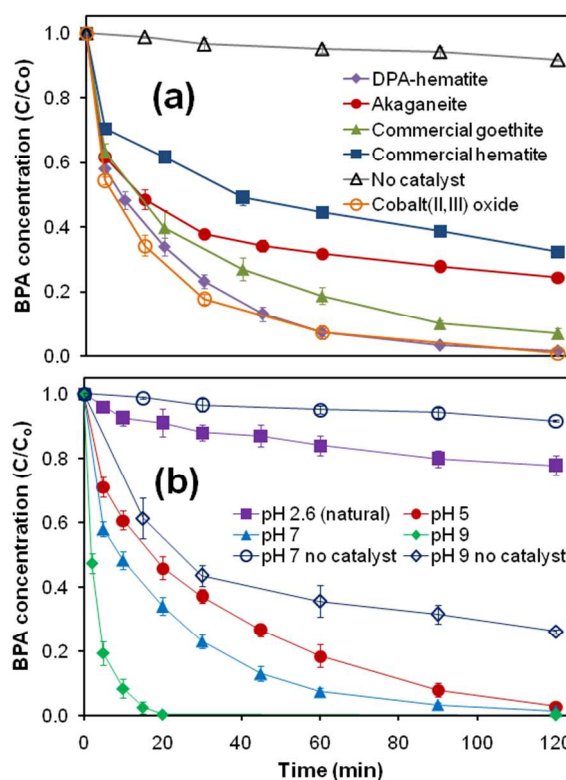
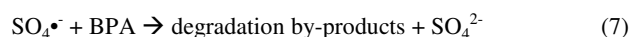
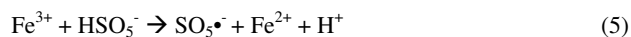


Fig 7. Effects of (a) different heterogeneous Fe(III) catalysts and (b) initial pH on BPA degradation. Conditions: $[\text{BPA}]_0 = 15 \text{ mg L}^{-1}$, $[\text{Oxone}]_0 = 2 \text{ g L}^{-1}$ and $[\text{catalyst}]_0 = 0.5 \text{ g L}^{-1}$.

alone. All the Fe(III)-based catalysts can activate oxone to degrade BPA. The surface Fe(III) of the catalyst acts as an electron acceptor and interconvert with Fe(II) in the presence of PMS to generate the freely-diffusible $\text{SO}_4^{\bullet-}$ and $\text{SO}_5^{\bullet-}$ as follows:¹³



The initial step involving the generation of the relatively weaker $\text{SO}_5^{\bullet-}$ radical by Fe(III) is the rate-determining step which functions to (i) minimize radical quenching effect, (ii) maximize the utilization of the generated radicals, and (iii) generate Fe(II) for $\text{SO}_4^{\bullet-}$ production.²⁴

The schematic illustration of the BPA detoxification process by DPA-hematite is shown in Fig. 8. The excellent performance of DPA-hematite over all the other Fe(III)-based catalysts was probably attributed to (i) the nano-sized structure of DPA-hematite which provides the highest surface area for reaction, and (ii) the presence of DPA functional groups on the surface of DPA-hematite. The surface OH- and DPA-functional groups act as σ -donor ligands and are beneficial in increasing the electron density and reactivity of Fe(III). While the commercial goethite achieved 90% of BPA removal within 120 min, it dissolved substantially during the 120-min reaction. The reaction system with DPA-hematite can be well described by the pseudo first-order kinetic model with the apparent rate constant, k_{app} , of 0.039 min^{-1} ($R^2 = 0.950$). However, the pseudo first-order kinetic model could not fit very well into reaction systems with the akaganeite, commercial hematite and commercial goethite due to the retardation of the BPA degradation towards the end of the reaction time which could be attributed to the deactivation of the catalyst and dissolution of Fe(III) as observed in the case of commercial goethite. The DPA-hematite was also compared with the commercial Co_3O_4 ($k_{app} = 0.041 \text{ min}^{-1}$, $R^2 = 0.946$). Comparable removal efficiency and rate were obtained with DPA-hematite being more environmentally-friendly and cost effective compare with Co_3O_4 , which suffers from Co leaching problem. Co leaching from Co_3O_4 is well-reported in the literature and the permissible limit for irrigation water is 0.05 mg L^{-1} (Environmental Bureau of Investigation, Canadian Water Quality Guidelines).^{14, 34, 35} However, a possible disadvantages of DPA-hematite is the possibility of oxidation of surface DPA during the catalytic reaction. In view of the eco-friendly nature of DPA-hematite coupled with its high catalytic activity, it was selected for further evaluation.

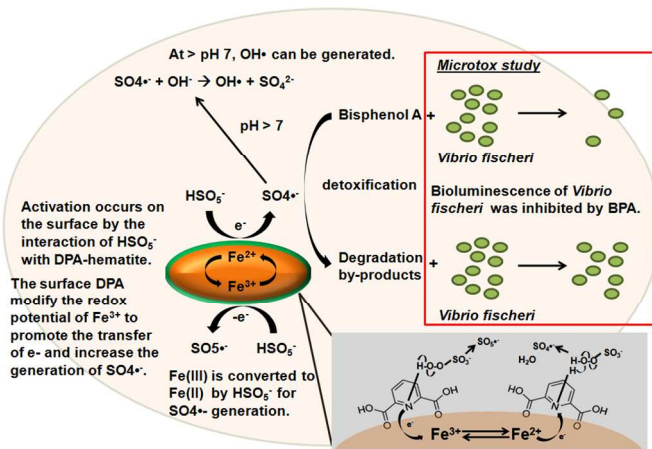


Fig 8. The schematic illustration of the BPA detoxification process by DPA-hematite.

Figure 7b presents the influence of initial pH (pH 2.6 – 9.0) on BPA removal. The BPA removal efficiencies were more than 95% within 120 min for all the initial pH studied except for pH 2.6 (natural pH) whereby only 22% of BPA was degraded. During the reaction, the pH change over 120-min was insignificant for the initial pH 2.6 and 5.0 while the final pH for initial pH 7.0 and 9.0 were 5.8 and 7.6, respectively. The pH_{zpc} of the DPA-hematite was pH 9.5 indicating that the surface charge of the DPA-hematite was

dominated by the positively-charged sites for the investigated pH range which was attributed to the enhanced surface protonation from the attached DPA ligand. The $\text{p}K_{a1}$ and $\text{p}K_{a2}$ of PMS are < 0 and 9.4, respectively, while the $\text{p}K_a$ for BPA is 9.6-10.2.^{36, 37} This appears to imply that the PMS species was in its negatively-charged state for the range of pH investigated. In this regard, the negatively-charged PMS should be favorably attracted to the catalytic sites of the DPA-hematite. However, at acidic pH condition, due to the occurrence of the PMS stabilization effect owing to the attachment of H^+ to the peroxide bond (O-O) of PMS, repulsion between PMS and the protonated catalytic sites (e.g. hydroxo and dipicolinate species) occurred.²⁵ This inhibited the PMS activation reaction resulting in the decrease in BPA degradation particularly at pH 2.6. The BPA removal rate increased with increasing pH, especially at pH 9.0 with all the BPA removed within 20 min and the highest k_{app} value of 0.262 min^{-1} . The excellent performance at pH 9.0 can also be ascribed to several factors. First, the presence of a relatively larger fraction of SO_5^- ions are relatively easier to be activated compare to PMS.³⁸ Second, under basic condition, more surface OH-groups are able to increase the electron density of the transition metal and act as σ -donor ligand which lowers the redox activation energy and increase the PMS activation reaction. Third, the electron mediation process generally increases with increasing pH due to the effective linkage of redox partners by bridged-surface ligand and OH-. Finally, the generation of the powerful OH^{\bullet} at pH 9 from the $\text{SO}_4^{\bullet-}$ (Eq. 8) could also accelerate the BPA removal.³⁹

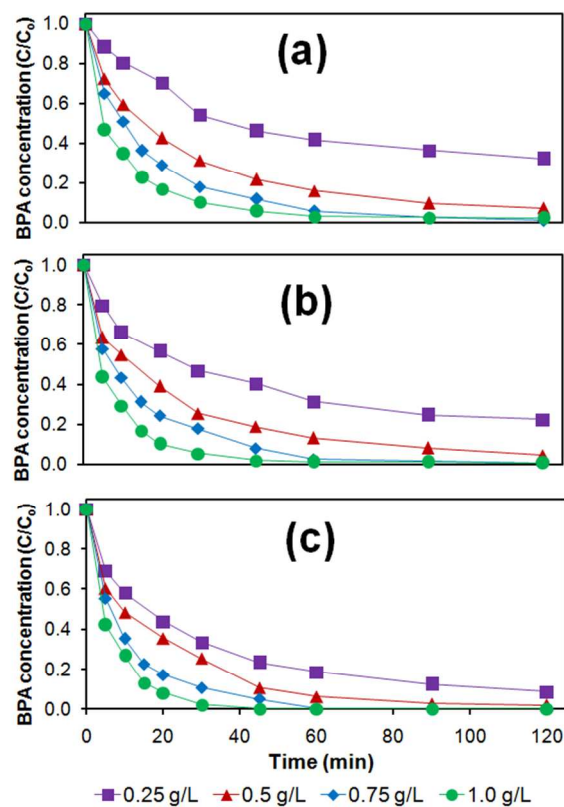
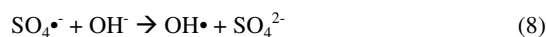


Fig 9. Effect of DPA-hematite loading on BPA degradation at oxone dosage of (a) 0.5, (b) 1.0 and (c) 2.0 g L^{-1} . Conditions: $[\text{BPA}]_0 = 15 \text{ mg L}^{-1}$, $\text{pH}_0 = 7$.

3.2.2 Effects of DPA-hematite loading and oxone dosage

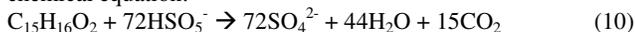
Figures 9 and 10 present the effects of DPA-hematite loading and oxone dosage on BPA degradation, respectively. The BPA removal can be expedited by increasing the DPA-hematite loading and oxone dosage. The higher amount of catalytic sites and reactant concentration were the reasons for the increase in reaction rate at various DPA-hematite loading and oxone dosages, respectively. The effects of catalyst loading and oxone dosage on reaction rate were more imperative at lower oxone dosage and catalyst loading, respectively. Since PMS activation reaction in the heterogeneous system is a surface phenomenon, the main prerequisite for the reaction to occur is the initial formation of a PMS-surface complex which is a diffusion- and equilibrium-driven processes. Under low catalyst loading and oxone dosage, limited PMS-surface contact was achieved. However, by increasing the oxone dosage, higher probability of PMS-surface contact would generate more $\text{SO}_4^{\bullet-}$ for BPA degradation. When catalyst loading was higher, there is abundance effective surface area for the initial formation of PMS-surface complex and the effect of oxone dosage became less important. Almost complete removal of BPA was observed within 120-min regardless of the oxone dosage used in this study when more than 0.5 g L⁻¹ of DPA-hematite was employed. To gain further insights into the influence of catalyst loading and oxone dosage on the BPA removal rate, the k_{app} coefficient is expanded to include the initial oxone concentration (D_o) and reaction surface area per unit volume (ρ_s) as follows:

$$-\frac{d[BPA]}{dt} = k_{app}[BPA] = k_{SD}[D_o]^{1/2}\rho_s[BPA] \quad (9)$$

where k_{SD} (L^{3/2} m⁻² g^{-1/2} min⁻¹) is the specific rate constant independent of the initial oxone dosage and catalyst loading. The assumption that the initial oxone concentration was in excess is valid considering the amount of oxone consumed for BPA removal was less than 20% and the oxone-to-BPA molar ratio is at least 12.5:1 (Section 3.3). Eq. 9 enables the estimation of k_{app} of the BPA removal rate at various initial oxone dosages and catalyst loadings at a given pH. The correlation between k_{app} with ρ_s and D_o can be established through fitting of Eq. (9) to the experimental data (k_{app}) using MATLAB, as shown in Fig. 11 whereby the k_{SD} value is 3.2×10^{-4} L^{3/2} m⁻² g^{-1/2} min⁻¹ ($R^2 = 0.95$) at pH 7.

3.3 Degree of mineralization and peroxymonosulfate consumption

The TOC removal data provides some useful insight into the degree of BPA mineralization while PMS consumption data provides information on the efficiency of the system in utilizing PMS during the course of BPA degradation. For complete oxidation of 15 mg L⁻¹ of BPA to carbon dioxide and water, the theoretical amount of oxone required is 1.45 g L⁻¹ which can be calculated from the following chemical equation:



The degree of mineralization and PMS consumption were investigated at oxone dosages of 0.5, 1.0 and 2.0 g L⁻¹ which encompass deficit (BPA to oxone molar ratio of 1:12.5 and 1:25) and excess (1:50) oxone conditions, all at 0.5 g L⁻¹ of DPA-hematite loading. Fig. 12 shows a strong influence of the oxone dosage on the degree of mineralization indicated as the TOC removal. Several organic acids, namely oxalic, acetic and formic acids were also detected at twofold concentration when 2.0 g L⁻¹ of oxone was used compared with 1.0 g L⁻¹. For all cases, despite more than 90% of BPA removed within 120 min, the degrees of mineralization were only 9±1, 21±4 and 38±2% for oxone dosages of 0.5, 1.0 and 2.0 g

L⁻¹, respectively, and the corresponding percentages of PMS consumed were only about 20% for all cases. The slower TOC removal and PMS consumption rates after 120 min were probably attributed to (i) the formation of recalcitrant aromatic BPA oxidation products that were resistant to further oxidation⁴⁰ and (ii) the blockage of the catalyst active sites due to the adsorption of the recalcitrant BPA intermediates. Nevertheless, after 24 h of reaction, the TOC removal efficiency increased significantly to 22, 42 and 67% for oxone dosages of 0.5, 1.0 and 2.0 g L⁻¹, respectively, suggesting that the temporal deactivation of catalyst surface was reversible. The calculated k_{SD} value for TOC removal using Eq. (9) at constant DPA-hematite loading and various initial oxone dosages was lower (2.6×10^{-5} L^{3/2} m⁻² g^{-1/2} min⁻¹) than the corresponding value for BPA removal attributed to the slower TOC removal.

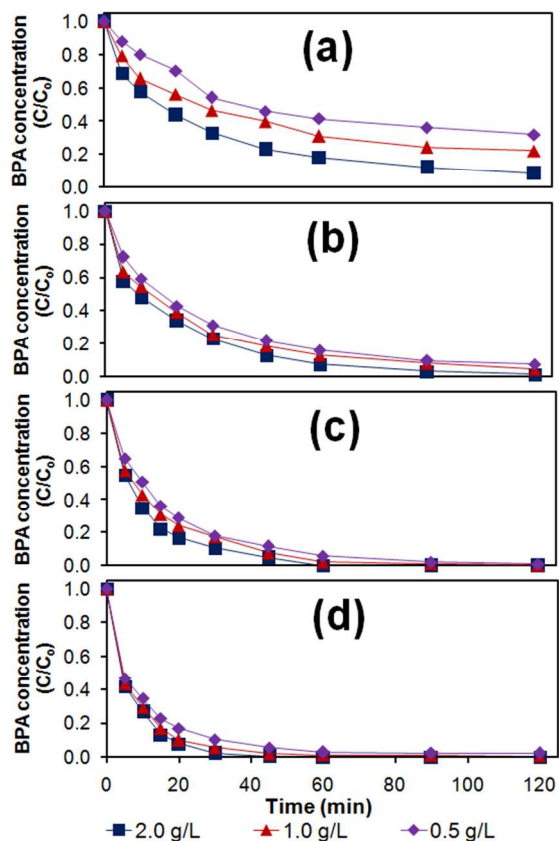


Fig 10. Effect of oxone dosage on BPA degradation at DPA-hematite loadings of (a) 0.25, (b) 0.50, (c) 0.75 and (d) 1.0 g L⁻¹. Conditions: $[BPA]_0 = 15 \text{ mg L}^{-1}$, $\text{pH}_0 = 7$.

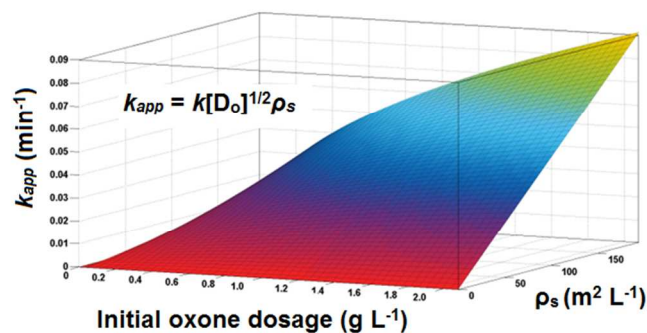


Fig 11. Relationship of k_{app} , ρ_s and initial oxone dosage at pH 7.

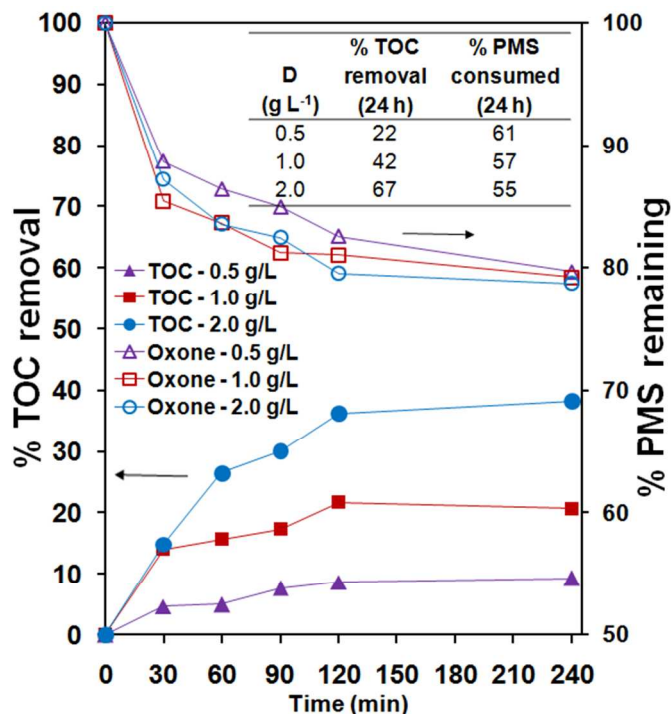


Fig 12. Time courses of TOC removal and PMS remaining at various initial oxone concentrations. Conditions: $[BPA]_0 = 15 \text{ mg L}^{-1}$, $\text{pH}_0 = 7$ and $[\text{catalyst}]_0 = 0.5 \text{ g L}^{-1}$.

3.4 Acute toxicity study

In view of the production of different recalcitrant BPA intermediates during the catalytic oxidation process which could be more toxic than BPA itself, the transient toxicity of BPA solution need to be evaluated. Hitherto, studies on the evolution of the acute toxicity of pollutants and their intermediates generated from S-AOPs are relatively rare, and most of which dealt with the persulfate system.^{41, 42} The intrinsic toxicity of PMS to microorganisms at elevated concentrations due to the high standard reduction potential of PMS ($E^\circ = 1.85 \text{ V}$) makes it difficult to evaluate the changes in acute toxicity of BPA intermediates over time using microbial bioassay. In this study, we presented a facile protocol to eliminate the toxicity interference induced by PMS by converting the residual PMS to innocuous sulfate ions through reaction with stoichiometric amount of Na_2SO_3 as follows:



After treatment of a blank oxone solution with Na_2SO_3 and followed by pH restoration to neutral, there was no significant difference ($p < 0.05$) in the acute toxicities based on *V. fischeri* of the blank DI water and oxone/ SO_3^{2-} solutions. Similar results were also obtained for the BPA and BPA/PMS/ SO_3^{2-} solutions. Furthermore, with the stoichiometric addition of SO_3^{2-} , PMS was not detectable using the iodometric method as mentioned in Section 2.7 while a stoichiometric amount of SO_4^{2-} ion was detected in the SO_3^{2-} treated solution. Thus, we employed this validated method that eliminates the PMS interference to investigate the transient toxicity of BPA solution during the course of reaction in the system.

The changes of inhibition of *V. fischeri* bioluminescence (at 5, 15 and 30 min of incubation time) induced by BPA and its degradation intermediates during the oxidation process at different oxone dosages are shown in Fig. 13. Although a similar trend was observed

for 5, 15 and 30 min of incubation time under the same condition, the acute toxicity patterns were greatly influenced by the oxone dosage. When 2.0 g L^{-1} of oxone (Fig. 13a) was employed, the percentages of inhibition generally increased from 79% at $t = 0 \text{ min}$ to 90% at $t = 90 \text{ min}$ probably due to the accumulation of toxic degradation intermediates such as succinic acid, 2,3-dimethyl benzoic acid and 3-hydroxy-4-methyl-benzoic acid which were generally more toxic than BPA itself.^{41, 43} However, the inhibitory effect was distinctively reduced after 90 min of treatment. This was attributed to the further degradation of the toxic intermediates to nontoxic organic acids as observed by the detection of acetic, formic and oxalic acids in our study using ion chromatography.

The changes in the transient toxicity of BPA solution when 0.5 g L^{-1} and 1.0 g L^{-1} of oxone were used can be explained in terms of the BPA intermediates produced during the oxidation process which undergo the dimerization and mineralization pathway as follow:^{44, 45}

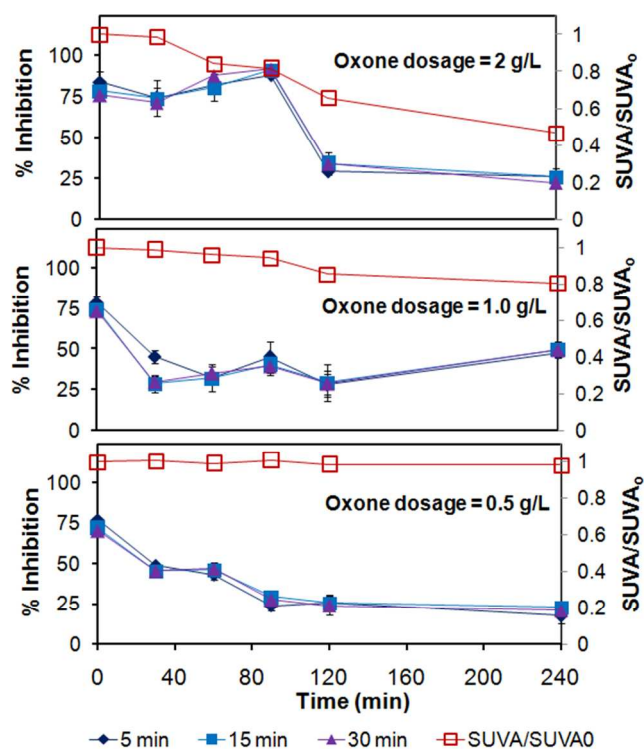
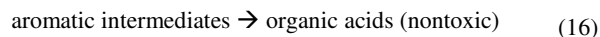
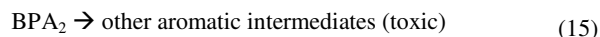
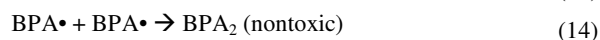
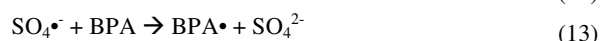
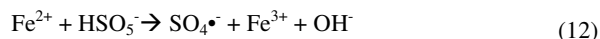


Fig 13. Time courses of acute toxicity and $\text{SUVA}/\text{SUVA}_0$ of BPA solution ($\pm \text{S.D.}$) during reaction at different initial oxone concentrations.

During the initial phase of degradation, higher molecular weight nontoxic intermediates were formed due to the dimerization reaction of BPA as observed by Hanci et al.⁴¹ Subsequent oxidation of the

higher molecular weight nontoxic intermediates resulted in the increased in toxicity of BPA solution. This was followed by the further transformation of toxic intermediates to nontoxic organic acids and finally to carbon dioxide and water. Considering that the amount of oxone consumed and TOC removal was inferior for 0.5 and 1.0 g L⁻¹ compared with 2.0 g L⁻¹ of oxone but the overall removal of BPA were also more than 95%, it can be implied that for cases with deficit oxone dosage (0.5 and 1.0 g L⁻¹), most of the BPA intermediates remain at the BPA₂ stage (Eq. 14). The specific UV absorbance (SUVA) or UV₂₅₄/DOC was determined (Fig. 13) to examine the extent of ring opening reactions. With 2.0 g L⁻¹ of oxone (Fig. 13a), decreased in intrinsic toxicity over time and ring opening reactions were observed supporting the fact that the mineralization was more complete. On the contrary, the SUVA analysis revealed that ring opening reactions were hardly observed when 0.5 g L⁻¹ of oxone was used which further substantiates the contention above. For the case of 1.0 g L⁻¹ of oxone, the results suggested slow conversion of BPA₂ to toxic aromatic intermediates at t = 120 min as indicated by the slow rise in the intrinsic toxicity. Therefore, based on the results, at the deficit oxone condition, it could be envisaged that toxic intermediates could be potentially accumulated in the treated water and excess oxone dosage is needed for achieving higher detoxification of BPA.

3.5 Reusability of DPA-hematite for BPA detoxification

Figure 14 shows the initial and final percentages of inhibition of the sample to the bioluminescence of *V. fischeri* and TOC removal efficiency for cycles 1, 2 and 3. The DPA-hematite can be reused by simple washing procedure without the need of undergoing tedious post-treatment procedure such as the post-calcination treatment as observed by Saputra et al. for α -Mn₂O₃.¹⁹ Marginal reduction of TOC removal efficiencies were observed over 3 cycles despite 95% of BPA was removed due to (i) unavoidable loss of catalyst during the catalyst recovery process which was estimated up to 11 % for each cycle and (ii) deactivation of the catalyst surface due to blockage of the catalyst surface and partial oxidation of DPA during catalytic reaction. Even so, the DPA-hematite can successfully detoxify BPA consistently (Fig. 14) without major change in removal efficiency giving indirect evidence that the DPA could still be retained after successive cycles. This shows that it was stable for BPA treatment and can be reused for at least 3 cycles.

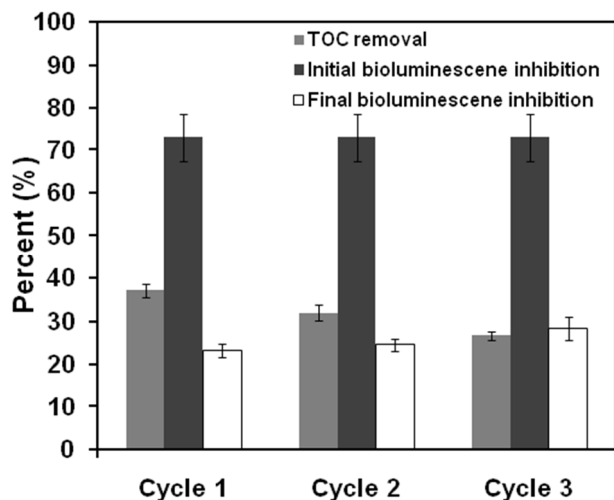


Fig 14. Total organic carbon removal efficiency and the corresponding initial and final inhibitions (\pm S.D.) for 3 cycles.

Conclusions

DPA-hematite with high surface area was successfully prepared by a facile urea-assisted co-precipitation of Fe-DPA⁺ complex to activate PMS for BPA degradation. The DPA-hematite performed remarkably better against other Fe(III)-based catalysts in BPA removal with PMS. The influence of oxone dosage was more pronounced at lower DPA-hematite dosage. Similarly, the influenced of DPA-hematite dosage was more important at lower oxone dosage. A simple predictive model was employed to predict the correlation between the rate constant and oxone dosages at various catalyst loadings. The change in transient toxicity of BPA solution during the course of reaction was successfully determined for the first time in PMS system at different oxone dosages. For detoxification of BPA, excess oxone condition needs to be employed to improve the mineralization of BPA. The DPA-hematite was stable and can be used to detoxify BPA for at least 3 cycles without any significant loss of its catalytic activity.

Acknowledgements

The authors would like to thank the Interdisciplinary Graduate School (IGS) and Nanyang Technological University (NTU) for the award of PhD research scholarship. The kind assistance from the laboratory staffs of Nanyang Environment and Water Research Institute (NEWRI) and Environmental Labs are gratefully acknowledged.

Notes and References

^aNanyang Environment and Water Research Institute (NEWRI), Nanyang Technological University, 1 Cleantech Loop, CleanTech One, Singapore 637141, Singapore. E-mail address: ctlim@ntu.edu.sg Tel: +65-6790 6933, Fax: +65-6791 0676

^bDivision of Environmental and Water Resources Engineering, School of Civil and Environmental Engineering, Nanyang Technological University, 50 Nanyang Avenue, Singapore 639798, Singapore.

^cSchool of Materials Science and Engineering, Nanyang Technological University, 50 Nanyang Avenue, Singapore 639798, Singapore.

- Subagio, D. P.; Srinivasan, M.; Lim, M.; Lim, T.-T., *Applied Catalysis B: Environmental* **2010**, *95*, 414-422.
- Rochester, J. R., *Reproductive Toxicology* **2013**, *42*, 132-155.
- Teeguarden, J. G.; Hanson-Drury, S., *Food and Chemical Toxicology* **2013**, *62*, 935-948.
- Metcalf, C. D.; Metcalf, T. L.; Kiparissis, Y.; Koenig, B. G.; Khan, C.; Hughes, R. J.; Croley, T. R.; March, R. E.; Potter, T., *Environmental Toxicology and Chemistry* **2001**, *20*, 297-308.
- Tsai, W.-T.; Lai, C.-W.; Su, T.-Y., *Journal of Hazardous Materials* **2006**, *134*, 169-175.
- Cajthaml, T.; Křesinová, Z.; Svobodová, K.; Möder, M., *Chemosphere* **2009**, *75*, 745-750.
- Nguyen, L. N.; Hai, F. I.; Yang, S.; Kang, J.; Leusch, F. D. L.; Roddick, F.; Price, W. E.; Nghiem, L. D., *Bioresource Technology* **2013**, *148*, 234-241.
- Keykavoos, R.; Mankidy, R.; Ma, H.; Jones, P.; Soltan, J., *Separation and Purification Technology* **2013**, *107*, 310-317.

9. Erjavec, B.; Kaplan, R.; Djinović, P.; Pintar, A., *Applied Catalysis B: Environmental* **2013**, *132–133*, 342-352.
10. Gao, B.; Lim, T. M.; Subagio, D. P.; Lim, T.-T., *Applied Catalysis A: General* **2010**, *375*, 107-115.
11. Olmez-Hanci, T.; Arslan-Alaton, I., *Chemical Engineering Journal*.
12. Matta, R.; Tlili, S.; Chiron, S.; Barbati, S., *Environ Chem Lett* **2011**, *9*, 347-353.
13. Anipsitakis, G. P.; Dionysiou, D. D., *Environmental Science & Technology* **2004**, *38*, 3705-3712.
14. Anipsitakis, G. P.; Stathatos, E.; Dionysiou, D. D., *The Journal of Physical Chemistry B* **2005**, *109*, 13052-13055.
15. Ding, Y.; Zhu, L.; Huang, A.; Zhao, X.; Zhang, X.; Tang, H., *Catalysis Science & Technology* **2012**, *2*, 1977-1984.
16. Shi, P.; Su, R.; Zhu, S.; Zhu, M.; Li, D.; Xu, S., *Journal of Hazardous Materials* **2012**, *229–230*, 331-339.
17. Zhang, W.; Tay, H. L.; Lim, S. S.; Wang, Y.; Zhong, Z.; Xu, R., *Applied Catalysis B: Environmental* **2010**, *95*, 93-99.
18. Shukla, P.; Wang, S.; Singh, K.; Ang, H. M.; Tadé, M. O., *Applied Catalysis B: Environmental* **2010**, *99*, 163-169.
19. Saputra, E.; Muhammad, S.; Sun, H.; Ang, H.-M.; Tadé, M. O.; Wang, S., *Applied Catalysis B: Environmental* **2013**, *142–143*, 729-735.
20. Saputra, E.; Muhammad, S.; Sun, H.; Patel, A.; Shukla, P.; Zhu, Z. H.; Wang, S., *Catalysis Communications* **2012**, *26*, 144-148.
21. Saputra, E.; Muhammad, S.; Sun, H.; Ang, H.-M.; Tadé, M. O.; Wang, S., *Journal of Colloid and Interface Science* **2013**, *407*, 467-473.
22. Ji, F.; Li, C.; Deng, L., *Chemical Engineering Journal* **2011**, *178*, 239-243.
23. Ji, F.; Li, C.; Wei, X.; Yu, J., *Chemical Engineering Journal* **2013**, *231*, 434-440.
24. Rastogi, A.; Al-Abed, S. R.; Dionysiou, D. D., *Applied Catalysis B: Environmental* **2009**, *85*, 171-179.
25. Zhang, T.; Zhu, H.; Croué, J.-P., *Environmental Science & Technology* **2013**, *47*, 2784-2791.
26. de Faria, E. H.; Ricci, G. P.; Marçal, L.; Nassar, E. J.; Vicente, M. A.; Trujillano, R.; Gil, A.; Korili, S. A.; Ciuffi, K. J.; Calefi, P. S., *Catalysis Today* **2012**, *187*, 135-149.
27. Uhrecký, R.; Padělková, Z.; Moncol, J.; Koman, M.; Dlháň, L. u.; Titiš, J.; Boča, R., *Polyhedron* **2013**, *56*, 9-17.
28. Halvorson, H.; Doi, R.; Church, B., *Proceedings of the National Academy of Sciences of the United States of America* **1958**, *44*, 1171-1180.
29. Anilkumar, G.; Bitterlich, B.; Gelalcha, F. G.; Tse, M. K.; Beller, M., *Chemical Communications* **2007**, 289-291.
30. Bridger, K.; Patel, R. C.; Matijević, E., *Polyhedron* **1982**, *1*, 269-275.
31. Crans Debbie, C.; Yang, L.; Gaidamauskas, E.; Khan, R.; Jin, W.; Simonis, U., Applications of Paramagnetic NMR Spectroscopy for Monitoring Transition Metal Complex Stoichiometry and Speciation. In *Paramagnetic Resonance of Metallobiomolecules*, American Chemical Society: 2003; Vol. 858, pp 304-326.
32. Pierre, J. L.; Fontecave, M., *Biomaterials* **1999**, *12*, 195-199.
33. García, K. E.; Barrero, C. A.; Morales, A. L.; Greneche, J. M., *Materials Chemistry and Physics* **2008**, *112*, 120-126.
34. Bhatnagar, A.; Minocha, A. K.; Sillanpää, M., *Biochemical Engineering Journal* **2010**, *48*, 181-186.
35. Chen, X.; Chen, J.; Qiao, X.; Wang, D.; Cai, X., *Applied Catalysis B: Environmental* **2008**, *80*, 116-121.
36. Staples, C. A.; Dome, P. B.; Klecka, G. M.; Oblock, S. T.; Harris, L. R., *Chemosphere* **1998**, *36*, 2149-2173.
37. Negri, A. R.; Jimenez, G.; Hill, R. T.; Francis, R. C., *Tappi journal* **1998**, *81*, 241-246.
38. Guan, Y.-H.; Ma, J.; Ren, Y.-M.; Liu, Y.-L.; Xiao, J.-Y.; Lin, L.-q.; Zhang, C., *Water Research*.
39. Mahdi Ahmed, M.; Barbati, S.; Doumenq, P.; Chiron, S., *Chemical Engineering Journal* **2012**, *197*, 440-447.
40. Huang, Y.-F.; Huang, Y.-H., *Journal of Hazardous Materials* **2009**, *167*, 418-426.
41. Olmez-Hanci, T.; Arslan-Alaton, I.; Genc, B., *Journal of Hazardous Materials*.
42. Liang, C.; Wang, C.-W., *Chemosphere* **2013**, *93*, 2711-2716.
43. Sánchez-Polo, M.; Abdel daiem, M. M.; Ocampo-Pérez, R.; Rivera-Utrilla, J.; Mota, A. J., *Science of The Total Environment* **2013**, *463–464*, 423-431.
44. Lau, T. K.; Chu, W.; Graham, N. J. D., *Environmental Science & Technology* **2006**, *41*, 613-619.
45. Khataee, A. R.; Mirzajani, O., *Desalination* **2010**, *251*, 64-69.

Title: High surface area DPA-hematite for efficient detoxification of bisphenol A via peroxymonosulfate activation

Table of Content entry:

DPA-hematite was synthesized by an eco-friendly one-step co-precipitation method for bisphenol A detoxification via peroxymonosulfate activation. Correlation between the initial oxone dosage, apparent rate constant and surface area was obtained. Acute toxicity study was conducted for the first time in the PMS system. The function of DPA in mediating the peroxymonosulfate activation is schematically illustrated.

Graphical Abstract

